Korean J. Chem. Eng., 36(6), 886-893 (2019)
DOI: 10.1007/s11814-019-0268-0

pISSN: 0256-1115
eISSN: 1975-7220

Sunset yellow degradation by ultrasound/peroxymonosulfate/$CuFe_2O_4$: Influential factors and degradation processes

Rouzhan Feizi*, Mehdi Ahmadi*,,†, Sahand Jorfi*,**,†, and Farshid Ghanbari*****

*Department of Environmental Health Engineering, Ahvaz Jundishapur University of Medical Sciences, Ahvaz, Iran
**Environmental Technologies Research Center, Ahvaz Jundishapur University of Medical Sciences, Ahvaz, Iran
***Department of Environmental Health Engineering, Abadan School of Medical Sciences, Abadan, Iran
(*Received 21 December 2018 • accepted 8 April 2019*)

Abstract−Sunset yellow (SY) dye removal from aqueous solution was assessed by ultrasound/peroxymonosulfate/$CuFe_2O_4$ nanoparticles. $CuFe_2O_4$ nanoparticles were synthesized and their properties were well determined by several advanced techniques. The effects of pH, catalyst dosage, peroxymonosulfate (PMS) concentration, and ultrasound (US) intensity were investigated on the decolorization. The best results (95.8% removal) were observed at pH=7, $CuFe_2O_4$= 25 mg/L, PMS=1.5 mM, US=200 W and 30 min. Nitrite and bicarbonate ions demonstrated high inhibition effect on the decolorization. PMS depicted high activity in the presence of $CuFe_2O_4$ compared to $S_2O_8^{2-}$ and H_2O_2. Around 40% reduction in the decolorization was observed in reusability experiments. Sulfate and hydroxyl radicals were the major species of SY degradation based on quenching experiments. A mineralization of 50% was obtained only in 30 min reaction time. This process can be effective for the destruction of organic dyes in colored wastewater.

Keywords: Azo Dyes, Sulfate Radical, Peroxymonosulfate, Copper Ferrite, Ultrasound

INTRODUCTION

The emission of wastewater from different industries containing various toxic chemical into the soil and water resources results in serious impacts [1]. Dyes are synthetic organic compounds applied in textile, leather, pharmaceutical, plastic, paint, and food industries. The largest class of synthetic dyes, with a variety of color and structure, are azo dyes (N=N) [2]. The solubility of most of azo dyes in water is so high which is easily absorbed by human body. Discharge of the dyes into the environment causes harmful effects on the ecosystem and humans. Thus, the removal of these dyes is necessary, prior to discharging into water resources [3,4]. There are several methods to remove dyes from industrial wastewater, including biological, physical and chemical processes. Biological methods are limited for the treatment of dye solutions due to toxicity of the dyes for microorganisms. Physical and chemical processes include coagulation and flocculation, ozonation, reverse osmosis, adsorption, and membrane filters [4]. However, these classic methods often lead to the production of high volume of sludge that has disposal and treatment problems. Furthermore, the operating cost of these methods is relatively very high. Advanced oxidation processes (AOPs) are efficient for the degradation of organic contaminants in aqueous media, producing highly reactive oxygen species (ROS), such as hydroxyl radicals ($^{\bullet}OH$) and sulfate radicals ($SO_4^{\bullet-}$) [5,6]. They destruct organic pollutants into harmless organic products and mineral matters. Sulfate radical ($SO_4^{\bullet-}$), in comparison with hydroxyl radicals ($^{\bullet}OH$), represents higher performance in contaminant degradation, because of the higher oxidative potential (2.5-3.1 V), longer half-life period (30-40 s) and high performance in wider range of pH (3-9) [7-9]. Sulfate radical ($SO_4^{\bullet-}$) is usually generated from persulfate (PS) and peroxymonosulfate (PMS) anions by different activators, such as heat [10], transition metals [11], UV [12], carbon-based catalyst [13] and ultrasound [14]. Compared to PS, PMS can be easily activated by transition metals, due to the asymmetric molecular structure. Therefore, PMS has exhibited a higher activation efficiency for most organic pollutants [15]. $SO_4^{\bullet-}$-based AOPs using PMS with a catalyst have emerged as a promising technique for the degradation of azo dyes [16]. Up to know, different heterogeneous catalysts have been synthesized and evaluated for the activation of PMS that are usually classified into metal oxide (Co_3O_4, $CuFe_2O_4$, Fe_2O_3 etc.) and supported metal oxide (Co_3O_4/MnO_2, $MnFe_2O_4$/graphene) catalysts [17].

Of those metal oxide catalysts, $CuFe_2O_4$ is a suitable activator for PMS with magnetic properties [18]. Spinel ferrites are known as MFe_2O_4 (M=Mn, Co, Ni, Mg), are the groups of magnetic substances which have been extensively applied in electronic purposes. They can be easily separated from the solution using magnetic fields. Ferrites have been applied for the activation of peroxygens in AOPs, thanks to their high hydroxyl surface groups and magnetic properties [18,19].

Nowadays, the combination of two or three activators has received great attraction for the application of AOPs in wastewater treatment [4]. In this way, the presence of US along with heterogeneous catalyst can be a new approach for enhanced degradation of organic pollutants. Indeed, ultrasonic waves in the presence of $CuFe_2O_4$ can accelerate PMS activation to produce sulfate radicals ($SO_4^{\bullet-}$). There is little information about the combination of US and spinel ferrites for PMS activation to treat organic pollutants.

†To whom correspondence should be addressed.
E-mail: Ahmadi241@gmail.com, sahand369@yahoo.com

Hence, the main goal of this study was the assessment of sunset yellow (SY) dye removal from aqueous solution by US/PMS/$CuFe_2O_4$ process. At first, nanoparticles were simply synthesized and their properties were determined. Influential factors, including pH, catalyst dosage, PMS concentration, US intensity on dye removal, were investigated. Reusability and stability of the catalyst and mechanism were also studied. The ideal goal of each chemical process for the elimination of organic compounds is the oxidation of mother molecule to mineral compounds. Hence, total organic carbon (TOC) has been often determined for this purpose. In this way, TOC removal and UV-vis spectrum were investigated to study mineralization degree.

MATERIALS AND METHODS

1. Chemicals

Oxone salt ($KHSO_5 \cdot 0.5KHSO_4 \cdot 0.5K_2SO_4$) was purchased from Sigma-Aldrich Inc. Sodium persulfate ($Na_2S_2O_8$), sodium chloride (NaCl), sodium nitrate ($NaNO_3$), sodium nitrite ($NaNO_2$), sodium sulfate (Na_2SO_4), sodium bicarbonate ($NaHCO_3$) were provided from Samchun Inc. Hydrogen peroxide (35%), sulfuric acid (98%), ethanol (EtOH) and tert-butyl alcohol (TBA) were purchased from Merck Co. Sunset yellow ($C_{16}H_{10}N_2Na_2O_7S$) was supplied from Alvan Sabet Company (Iran) with 99% purity. The chemical structure and characteristics of sunset yellow dye are given in Table 1.

2. Preparation of $CuFe_2O_4$ Nanoparticles

$CuFe_2O_4$ was synthesized according to co-precipitation method [20]. In brief, $Cu(NO_3)_2 \cdot 3H_2O$ (0.025 M) and $Fe(NO_3)_3 \cdot 9H_2O$ (0.05 M) were dissolved in 100 mL distilled water, which was followed by slow addition of 75 mL NaOH (4.0 M) into solution and heating at 90 °C and finally the stirring was stopped. Then, the suspension was kept in quiescent conditions during 2 h at 90 °C. After cooling, filtration and washing using distilled water were conducted followed by drying at 80 °C overnight.

3. Characterization of $CuFe_2O_4$ Nanoparticles

The morphology of the copper ferrite was examined by field emission scanning electron microscopy (FESEM) (Mira 3-XMU) equipped with an energy dispersive X-ray spectrometer (EDS). X-ray diffraction (XRD) pattern was obtained using a Quantachrome/NOVA 2000X-ray diffractometer with a graphite monochromatic Cu $K\alpha$ radiation (λ=1.54 Å) at the accelerating voltage 40 kV and the current 30 mA over the 2θ scanning range of 10-80°. The Brunauer-Emmett-Teller (BET) surface area was measured by N_2 adsorption–desorption isotherm analysis at 77 K (TriStar II Plus, USA). UV-Vis diffuse reflectance spectroscopic (DRS) study was obtained under atmospheric conditions using a UV-vis spectrophotometer (UV3010, Hitachi) in the range of 190 nm to 800 nm. A vibrating sample magnetometer (VSM, 7400, Lakeshare, USA) was applied for measuring the magnetization at room temperature (25±1 °C).

Table 1. Chemical structure and characteristics of sunset yellow

Dye	Sunset Yellow
Commercial name	E110
Systematic name	Disodium6-hydroxy-5-[(4- sulfophenyl)azo] 2-naphthalenesulfoate
Chemical structure	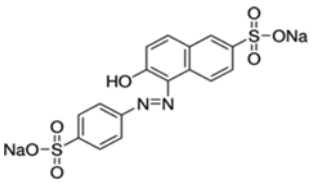
Formula	$C_{16}H_{10}N_2Na_2O_7S_2$
Molecular weight	452.36 g·mol^{-1}
Color index no.	15985

4. Experimental Procedures

A standard beaker was used as a reactor vessel for all experiments. The experiments were at atmospheric temperature and pressure. 100 mL dye solution was added into reactor. 1 N sodium hydroxide and sulfuric acid solutions were applied for adjusting solution pH. Constant amounts of catalyst $CuFe_2O_4$ and PMS were added to 100 mL of dye solution. Afterwards, these suspensions were placed in an ultrasound apparatus. The ultrasonic irradiation was provided using a laboratory homogenizer ultrasonic 0-400 W (Ultrasonic Technology Development Company, Iran). The experiments were also carried out at the different pH levels to explain the influence of solution pH on the decolorization of SY. Also, tests with catalyst doses (0 to 200 mg/L), PMS (0 to 2 mM), and the effect of ultrasound power (100 to 400 W) were performed to determine the optimal conditions for SY removal. The $CuFe_2O_4$ was collected from the solution using a magnet.

5. Analytical Method

Residual dye concentrations were determined using a UV/Vis spectrophotometer (DR-5000, HACH, USA) at the absorbance peak wavelength of 482 nm. The removal efficiency of SY (%) was obtained with Eq. (1):

$$\text{SY removal}\,(\%) = \frac{C_0 - C_t}{C_0} \times 100 \quad (1)$$

where C_0 is the initial SY concentration, C_t is the SY concentration at times. A TOC analyzer instrument (Shimadzu VCHS/CSN, Japan) was applied for the measurement of total organic carbon (TOC). Iron and copper leaching were measured by an atomic absorption spectrometer (Analytik Jena AG, Jena, Germany).

RESULTS AND DISCUSSION

1. Characterizations of $CuFe_2O_4$ Nanoparticles

Fig. 1(a) shows the FESEM image for $CuFe_2O_4$ nanocatalysts. According to Fig. 1(a), $CuFe_2O_4$ has an erratic morphology with rough cubic form with high agglomeration. The average particle size diameter of nanocatalyst was in range of 14-26 nm, confirming that copper ferrite particles were in nanoscale. The appearance of Cu and Fe with 1 : 1.8 ratio in EDS analysis was close to the 1 : 2 theoretical ratio in $CuFe_2O_4$ structure, confirming high function of co-precipitation method. In addition, no impurity peaks were observed in EDS spectrum (Fig. 1(b)), demonstrating high purity of synthesized nanocatalyst. The purity of $CuFe_2O_4$ is illustrated in the XRD spectrum, which is in line with the patterns of standards based on their JCPDS cards. According to Fig. 1(c), six peaks were observed at 2θ of 18.5°, 30.2°, 35.8°, 43.03°, 57.05° and

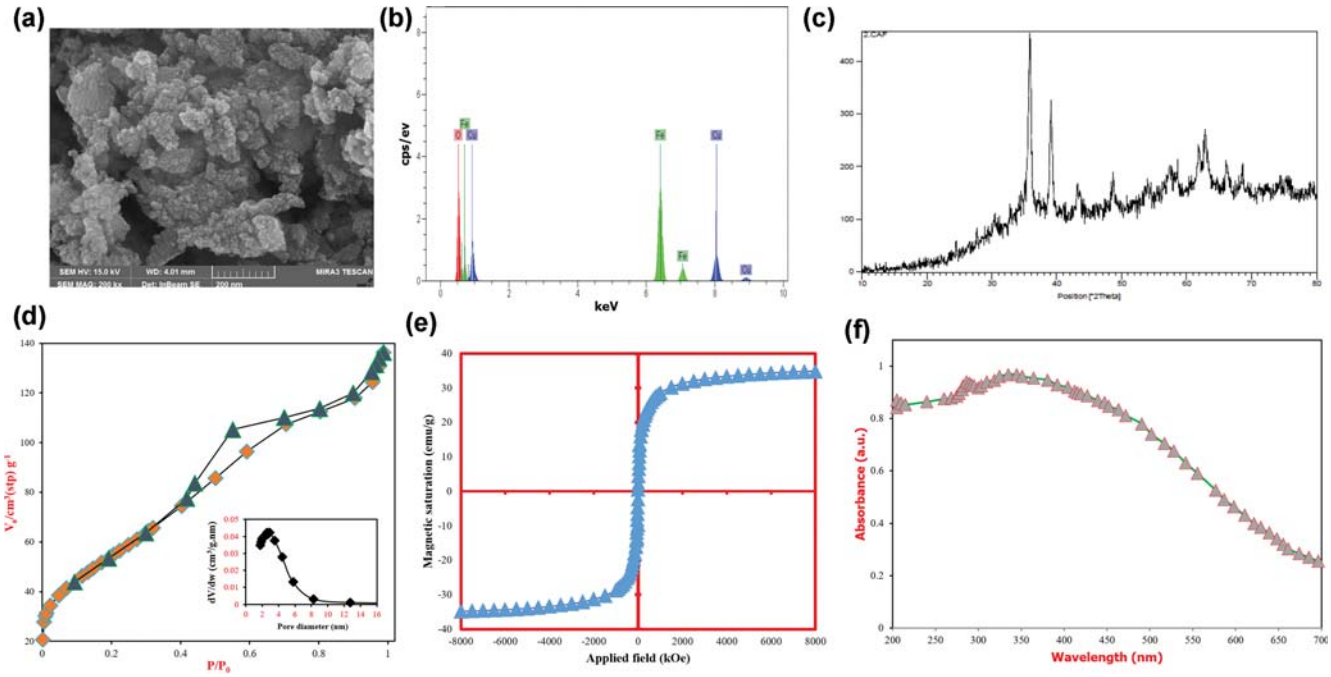

Fig. 1. Characteristics of $CuFe_2O_4$ (a) FESEM, (b) EDS, (c) XRD patterns, (d) N_2 adsorption-desorption isotherms, (e) magnetic hysteresis loops and (f) UV-Vis absorption spectra.

62.8° which can be related to the cubic phase of $CuFe_2O_4$ (JCPDS no. 25-0283), from planes (111), (220), (311), (400), (511) and (440), respectively [21]. The high degree of crystallization of copper ferrite was marked by narrow and strong diffraction peaks. The average size of 16.7 nm was obtained for $CuFe_2O_4$, according to Debye-Scherrer formula. The pore size distribution of $CuFe_2O_4$ obtained by N_2 adsorption/desorption is shown in Fig. 1(d). A mesoporous structure along with a hysteresis loop was observed for copper ferrite using typical Langmuir type IV isotherms. Results showed that average of pore size of $CuFe_2O_4$ was 2.6 nm. The mesoporous structure of $CuFe_2O_4$ nanocatalysts caused larger BET surface (201.89 m^2/g) and total pore volume (0.19 cm^3/g) (Table 2). The mesoporous structure and larger surface area provide a larger number of reactive sites, which improves the ability of catalysts to surface reaction with PMS and SY.

The ferromagnetic characteristics of $CuFe_2O_4$ was displayed by magnetic hysteresis loops (Ms=33.2 emu/g), indicating that $CuFe_2O_4$ can be simply separated by a magnet (Fig. 1(e)). According to UV-visible spectrum of $CuFe_2O_4$ nanocatalyst (Fig. 1(f)), a large amount of absorption was seen between UV and visible region, which was in agreement with another study [22]. Accordingly, a shift was observed in the $CuFe_2O_4$ nanocomposite absorption peaks between 190 and 800 nm range. As can be seen, copper ferrite showed the ability of absorption of light energy in UV and visible regions, which can be an advantage in terms of photo-activity.

Table 2. Physiochemical properties of $CuFe_2O_4$

Characteristics	Values
S_{BET} (m^2/g)	201.89
Total pore volume (cm^3/g)	0.19
Average pore diameter (nm)	2.6
Pore structure	Mesoporous
Color	Black

2. Effect of operating parameters on the PMS/$CuFe_2O_4$/US Process

One of the most important factors in the degradation of dye during the oxidation reaction is solution pH. Heterogeneous AOP_s can be operated on a broad pH range, but always have a better performance in slightly acidic or neutral conditions [23,24]. The influence of initial solution pH on the performance on US/PMS/$CuFe_2O_4$ for SY degradation was examined under the conditions of SY concentration 50 mg/L, $CuFe_2O_4$ 100 mg/L, PMS 1.0 mM, and US 200 W (Fig. 2(a)). The results showed that the highest efficiency of SY removal was at pH=7.0 in the PMS/$CuFe_2O_4$/US process. At this pH, after 30 min reaction time, the removal efficiency was 88.5%. In high acidic conditions (pH=2.0), a decrease was observed in decolorization (66% removal efficiency); this circumstance has been previously reported in some studies. Theoretically, high proton concentrations (H^+) scavenge sulfate radicals based on Eq. (2) [4,25].

$$SO_4^{\bullet-} + H^+ + e^- \rightarrow HSO_4^{\bullet-} \quad (2)$$

This hybrid process illustrates high efficiency in a wide range of pH (4.0-11.0), proving that the process can be used for the treatment of a variety of industrial effluents. Similar results have been reported in lopromide removal using $CuFe_2O_4$ activated PMS system [26]. Thus, pH of 7.0 was selected as an optimum pH for the next experiments.

The effect of catalyst dosage on the SY degradation was studied by US/PMS/$CuFe_2O_4$ (Fig. 2(b)). To optimize catalyst dosage, the

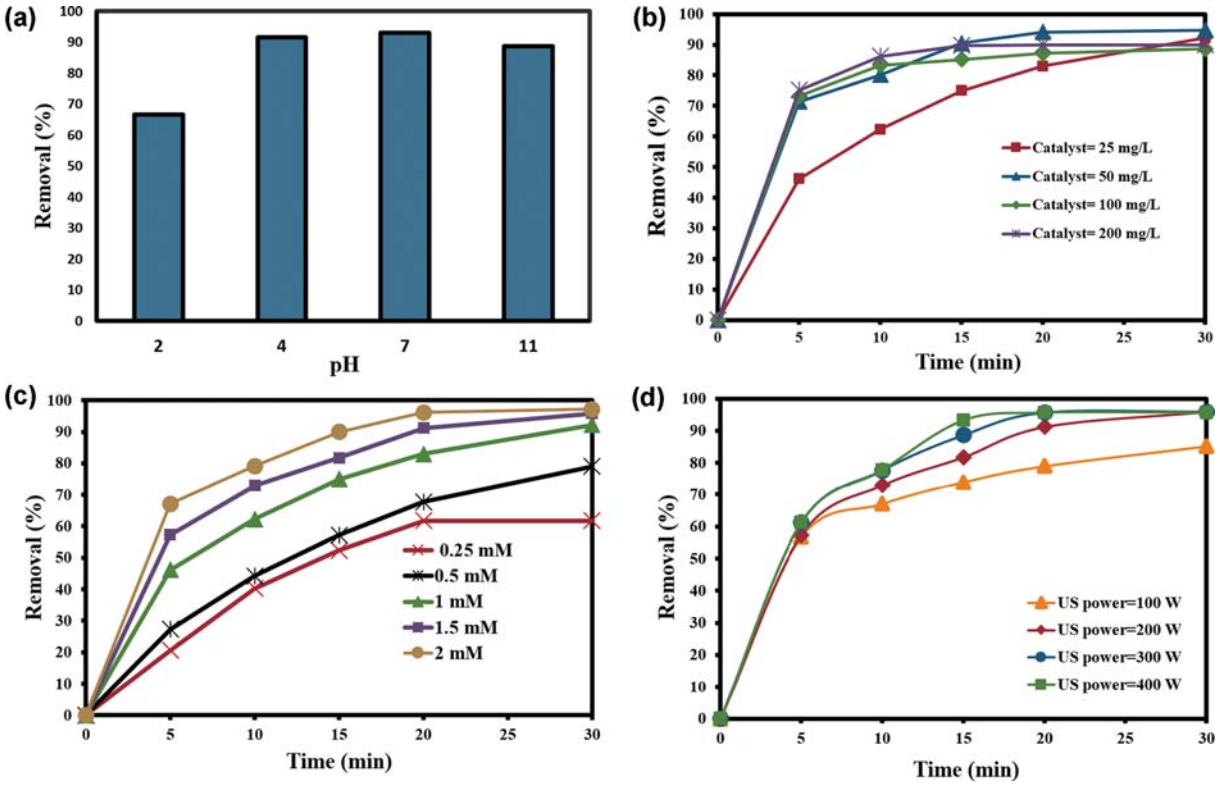

Fig. 2. (a) The effect of initial solution pH on SY removal in PMS/$CuFe_2O_4$/US process (SY=50 mg/L, $CuFe_2O_4$=100 mg/L, PMS=1 mM, US= 200 W), (b) The effect of catalyst dose on SY removal in PMS/$CuFe_2O_4$/US process (SY: 50 mg/L, pH=7, PMS=1 mM, US=200 W), (c) the effect of PMS on SY removal in PMS/$CuFe_2O_4$/US process (SY=50 mg/L, PMS=1.5 mM, $CuFe_2O_4$=25 mg/L, pH=7, US=200 W) (d) the effect of ultrasonic power on SY removal in PMS/$CuFe_2O_4$/US process (SY=50 mg/L, PMS=1.5 mM, $CuFe_2O_4$=25 mg/L, pH=7).

$CuFe_2O_4$ dosage was varied between 25, 50, 100 and 200 mg/L. According to Fig. 2(b), although the increase of catalyst loading from 25 mg/L to 50, 100 and 200 mg/L enhanced the decolorization rate, desirable decolorization (92%) was obtained at the lowest level (25 mg/L) during 30 min reaction time. The increasing dosage of $CuFe_2O_4$ supplied more active sites on the surface of $CuFe_2O_4$, that could expedite reactions to produce more free radicals, causing an enhancement in removal efficiency. In addition, the lower degradation efficiency for higher copper ferrite dosage (200 mg/L) would be explained by insufficient consumption of PMS due to agglomeration of catalyst at a large amount of copper ferrite [27]. Hence, the optimum catalyst dosage was selected as 25 mg/L for the dye degradation.

The effect of PMS concentrations (0-2 mM) on process performance was evaluated in US/PMS/$CuFe_2O_4$ system for the degradation of SY (Fig. 2(c)). Results clearly showed that the enhancement of dye removal efficiency was observed, by an increase in PMS concentration. The highest SY removal in US/PMS/$CuFe_2O_4$ process (97.20%) was seen at PMS=2 mM after 30 min of reaction time. It could be deduced that PMS is the main origin of the reactive sulfate radicals increasing the generation of reactive species at high PMS dosages. It has been reported that by increasing the oxidizing dosage concentration, higher radicals were produced, leading to higher dye removal [16,28]. However, the performance of the process in 1.5 mM PMS was similar to 2 mM PMS. These outcomes showed that excessive PMS did not result in scavenging effect.

The influence of different ultrasonic power (100 to 400 W) on the performance of US/PMS/$CuFe_2O_4$ was examined for the degradation of SY under the conditions of SY 50 mg/L, $CuFe_2O_4$ 25 mg/L and PMS 1.5 mM (Fig. 2(d)). By an increase in ultrasonic power between 100 and 200 W, an improvement was observed in removal efficiency from 85% to 95%. However, additional enhancement in ultrasonic power up to 400 W did not lead to improvement of dye degradation efficiency. It could be deduced that at high ultrasonic power, a portion of ultrasonic power would be consumed and converted to heat, because of the existence of scattering effect [29]. Therefore, US power 200 W was a suitable condition for US/PMS/$CuFe_2O_4$ process.

3. Degradation of SY in the Different Systems

Fig. 3 shows the degradation of SY at different systems. Results indicated that in a control test with only ultrasound, almost negligible (1%) color removal was obtained after 30 min, which can be ascribed to the lack of formation of $HO^{\bullet}$. In the control test with only $CuFe_2O_4$ (25 mg/L), about 5.88% dye removal was obtained after 30 min owing to the adsorption on the catalyst surface. The application of PMS alone (1.5 mM) induced about 12% dye removal as a result of direct oxidation by PMS. By simultaneous application of ultrasound and PMS, the degradation of dye was enhanced (39%) based on following equations. In fact, US can destruct O-O

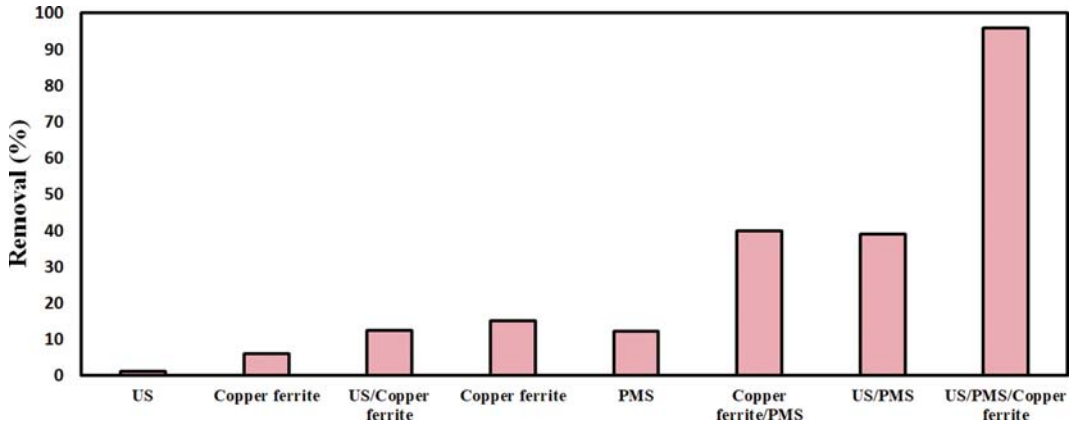

Fig. 3. Degradation of SY in the different systems ($CuFe_2O_4$=25 mg/L, pH=7, PMS=1.5 mM, US=200 W and time=30 min).

bond of PMS to generate free radicals. Moreover, hydrogen radical as a powerful reductive agent (E^0=−2.3 V), which is produced from sonolysis of water, can activate PMS for the generation of sulfate radical (Eq. (5)) [25].

$$HSO_5^- + US \rightarrow SO_4^{\bullet-} + HO^{\bullet} \quad (3)$$

$$H_2O+))) \rightarrow HO^{\bullet} + H^{\bullet} \quad (4)$$

$$HSO_5^- + H^{\bullet} \rightarrow SO_4^{\bullet-} + H_2O \quad (5)$$

When catalyst was combined with the US, only little dye removal (12%) was obtained after 30 min, because small quantities of reactive radicals were generated in the absence of PMS. PMS/$CuFe_2O_4$ could degrade 38% of SY after 30 min reaction time. In fact, Fe(III) and Cu(II) were the main agents of PMS activation to produce sulfate radical. 96% of SY was abated by PMS/$CuFe_2O_4$/US, indicating that the combination of US and $CuFe_2O_4$ for PMS activation was an effective method. In this way, $CuFe_2O_4$ can activate PMS through following reactions [30]. Ternary system (PMS/$CuFe_2O_4$/US) indicated that concurrent use of two activators was a synergistic manner for free radical production from PMS decomposition.

$$\equiv Cu(I) + HSO_5^- \rightarrow \equiv Cu(II) + OH^- + SO_4^{\bullet-} \quad (6)$$

$$\equiv Cu(II) + HSO_5^- \rightarrow \equiv Cu(I) + H^+ + SO_5^{\bullet-} \quad (7)$$

$$\equiv Fe(III) + HSO_5^- \rightarrow \equiv Fe(II) + SO_5^{\bullet-} + H^+ \quad (8)$$

$$\equiv Fe(II) + HSO_5^- \rightarrow \equiv Fe(III) + SO_4^{\bullet-} + OH^- \quad (9)$$

Moreover, US can regenerate Cu(II) and Fe(III) to lower valances of them (Cu(I) and Fe(II)) to accelerate sulfate radical production based on Eq. (10).

$$\equiv Cu(I) + Fe(III) \xrightarrow{US} \equiv Cu(II) + Fe(II) \quad (10)$$

Moreover, US irradiation has demonstrated that is a cleaning agent for the surface of catalysts. Indeed, US irradiation can remove impurities formed on $CuFe_2O_4$ nanoparticles to prevent deactivation [31].

4. Comparison of PMS with Persulfate and Hydrogen Peroxide

Hydrogen peroxide (HP), persulfate (PS) and PMS have been extensively used for the degradation and treatment of several organic pollutants and contaminated water in recent years [32]. SY removal was studied in PMS/$CuFe_2O_4$/US, PS/$CuFe_2O_4$/US, HP/$CuFe_2O_4$/US systems (Fig. 4(a)). Although previous studies reported that $CoFe_2O_4$ could decolorize methylene blue at 4 mL HP in 120 min [33]; however, in the current study, HP/$CuFe_2O_4$/US showed almost no SY removal. The activation of HP on $CuFe_2O_4$ may occur during the long reaction time and high dosage of HP. Therefore, it is obvious that H_2O_2 cannot be activated completely on $CuFe_2O_4$ surface. PS was also ineffective for SY removal in current system.

It is apparent that HP and PS cannot be activated completely on

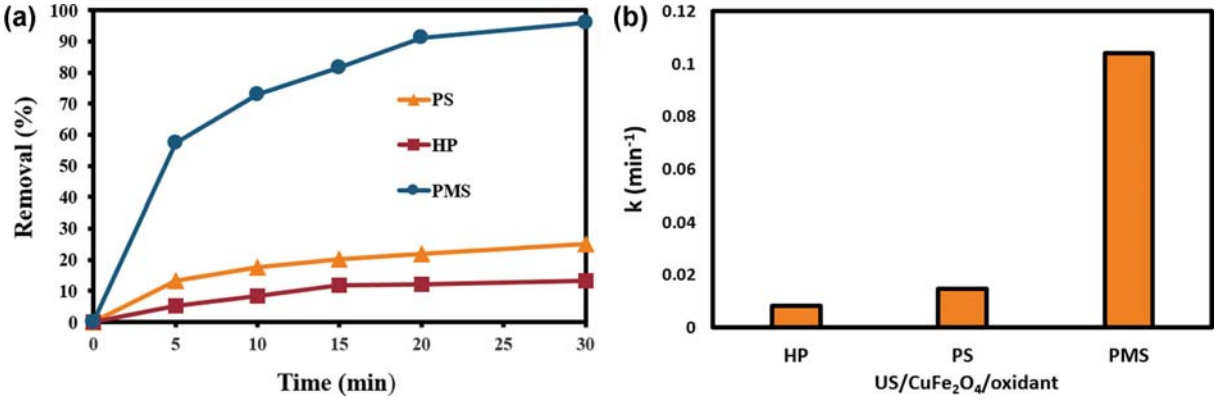

Fig. 4. The effect of different peroxides on the $CuFe_2O_4$/US process (a) decolorization (b) rate constants (SY=50 mg/l, pH=7, PMS=1.5 mM, US: 200 W).

$CuFe_2O_4$ surface. Symmetrical structure of HP and PS can be a rational reason for resistance to the activation. In fact, the dissociation of O-O bond is more difficult in PS and HP compared to PMS. Similar findings have been reported by Anipsitakis and Dionysiou [34].

The reaction rate of SY decolorization was studied using a first-order kinetic model according to Eq. (11):

$$\ln\frac{[SY]}{[SY]_0} = -kt \quad (11)$$

where, SY_0 and SY_t represent the concentrations of SY at time 0 and t, respectively. k is the reaction rate constant and t is reaction time. k value is obtained from calculation of line slop resulting from plot of ln (SY/SY_0) *vs* t (Fig. 4(b)). The rate constant (k) values for PMS/$CuFe_2O_4$/US, PS/$CuFe_2O_4$/US, HP/$CuFe_2O_4$/US were obtained 0.1041, 0.0147 and 0.0082 min^{-1} respectively. As can be seen, the rate constant of PMS process was ten times higher than that of PS and HP processes.

5. The Effect of Co-existing Anions on the PMS/$CuFe_2O_4$/US Process

The presence of different anions may affect the efficiency in sulfate radicals-based advanced oxidation processes (SR-AOPs) by scavenging effect. Therefore, in this study, we examined the effects of several inorganic anions (Cl^-, NO_3^-, NO_2^-, HCO_3^- and SO_4^{2-}) on SY degradation in PMS/$CuFe_2O_4$/US process. As shown in Fig. 5, the presence of anions led to the inhibition of SY degradation. In the presence of anions, the decolorization rate followed from this order: $SO_4^{2-} \le HCO_3^- < Cl^- < NO_3^- < NO_2^-$.

Bicarbonate ions have been identified as inhibition agents in AOPs. Rate constants of bicarbonate ions with sulfate and hydroxyl radicals are relatively high [35]. Hence the presence of bicarbonate ions can eventuate a competition for reaction with free radicals. Moreover, it has been reported that the reaction of PMS with bicarbonate ion can lead to the formation of peroxymonocarbonate anion (HCO_4^-). Chloride ions can reduce the efficiency of SR-AOPs through two ways: scavenging of hydroxyl and sulfate radicals; and by direct reaction with PMS according to Eqs. (12) and (13) [36,37].

$$Cl^- + HSO_5^- \rightarrow SO_4^{2-} + HOCl \quad (12)$$

$$2Cl^- + HSO_5^- + H^+ \rightarrow SO_4^{2-} + Cl_2 + H_2O \quad (13)$$

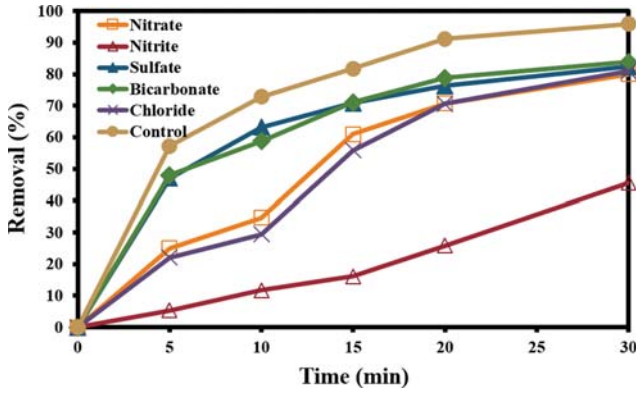

Fig. 5. The effect of different anions on the PMS/cuFe_2O_4/US process (SY=50 mg/L, pH=7, PMS=1.5 mM and US: 200 W).

In the presence of nitrate ions, nitrate radical ($NO_3^{\bullet}$) can be produced based on Eq. (14) in which sulfate and hydroxyl radical were scavenged by nitrate ions in aqueous solution.

$$NO_3^- + SO_4^{\bullet-} \rightarrow NO_3^{\bullet} + SO_4^{2-} \quad (14)$$

Nitrite ion has been well-known as a reducing and strong scavenging agent in chemical oxidation processes. As can be seen, high inhabitation effect occurred in the presence of nitrite ion in which 45% decolorization was obtained. Besides the role of scavenging of nitrite ion, nitrite ion can directly react with PMS. Hence, PMS as precursor of free radicals is eliminated from chain reactions of the activation by US and $CuFe_2O_4$ (Eq. (15)). The higher inhibition degree in SY degradation in the presence of NO_2^- may be due to the competition between nitrite and SY, NO_2^- acts as free radical scavenger for reaction with the oxidizing species hindering the degradation of SY [38].

$$NO_2^- + HSO_5^- \rightarrow NO_3^- + HSO_4^- \quad (15)$$

6. Quenching Experiments in PMS/$CuFe_2O_4$/US System

Ethanol (EtOH) and *tert*-butyl alcohol (TBA) were used as radical scavengers to identify the oxidizing radical species in PMS/$CuFe_2O_4$/US system. Ethanol reacts with $HO^{\bullet}$ and $SO_4^{\bullet-}$ at the rate constants of 1.6-7.7×10^7 $M^{-1}s^{-1}$ and 1.2-2.8×10^9 $M^{-1}s^{-1}$, respectively. TBA is a particular scavenger for $HO^{\bullet}$ with a rate constant of 7.6×10^8 $M^{-1}s^{-1}$, while its rate constant with sulfate radical is 4×10^5 M^{-1} s^{-1}, which is one-thousand times less than hydroxyl radical [4,25, 39]. A series experiments were conducted on SY removal by PMS/$CuFe_2O_4$/US system in the presence of TBA and EtOH (100 mM) and their rate constants are presented in Fig. 6. The results clearly indicated that EtOH markedly inhibited the dye degradation rate (k=0.0274 min^{-1}) by PMS/$CuFe_2O_4$/US, demonstrating that both sulfate and hydroxyl radical were major agents of dye degradation. On the other hand, TBA had an inhibitory effect on dye decolorization rate (k=0.0475 min^{-1}). Regarding the results of scavenging experiments with EtOH and TBA, it can be claimed that both hydroxyl and sulfate radicals had the same role in the degradation of dye. The contribution of hydroxyl radical can be due to the reaction of sulfate radical with water molecule (Eq. (16)). Moreover, the combination of two molecules of $SO_5^{\bullet-}$ can lead to the formation of hydroxyl radical ($HO^{\bullet}$) in the surface of $CuFe_2O_4$ (Eq. (17)) [26].

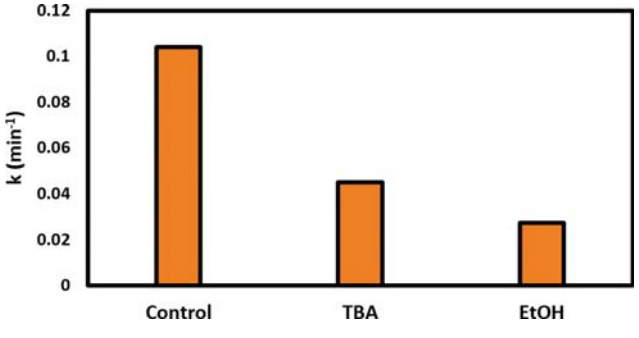

Fig. 6. The effect of scavengers (TBA and EtOH) on rate constant in the PMS/$CuFe_2O_4$/US process (SY: 50 mg/L, pH=7, PMS=1.5 mM, US=200 W and TBA and EtOH=100 mM).

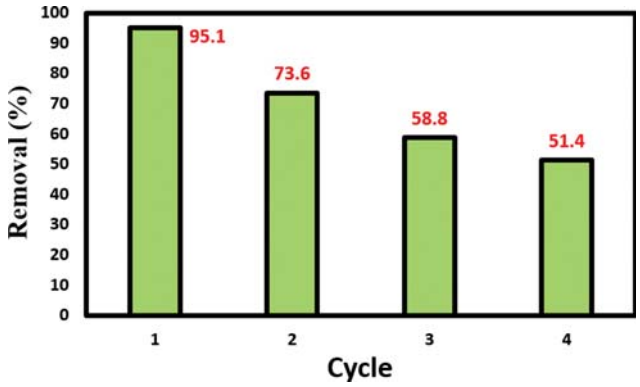

Fig. 7. Influence of cycle runs on SY degradation using by PMS/$CuFe_2O_4$/US process (SY=50 mg/L, $CuFe_2O_4$=25 mg/L, pH=7, PMS=1.5 mM, US=200 W and time=30 min).

Scheme 1. The schematic mechanism of SY degradation by PMS/$CuFe_2O_4$/US process.

$$SO_4^{\bullet-} + H_2O \rightarrow SO_4^{2-} + HO^{\bullet} + H^+ \quad (16)$$

$$2{\equiv}Cu(II) - SO_5^{-\bullet} + 2H_2O \rightarrow 2{\equiv}Cu(II) - HO^{\bullet} + O_2 + 2SO_4^{2-} + 2H^+ \quad (17)$$

7. Stability and Reusability of $CuFe_2O_4$

Stability is important for catalysts in industrial implications. An external magnet would be enough for the separation of this catalyst from solution, thanks to the magnetic features. To assess the stability of $CuFe_2O_4$, nanoparticles were collected and recycled at room temperature. The catalysts were separated, washed and recycled for four times. According to Fig. 7, dye degradation efficiencies were 95.1, 73.3, 58.8 and 51.4% for first to fourth runs, respectively. These results showed that $CuFe_2O_4$ catalyst lost the efficiency about 40% during four cycles without any regeneration method. Two reasons can be given for this phenomenon: first, the deactivation of catalyst surface by occupation of active site with intermediates; second, the agglomeration of nanoparticles after each run due to magnetic property.

The concentrations of Cu and Fe were measured after four cycles. The concentrations of Cu and Fe were obtained 1.0 and 0.9 mg/L, respectively. Indeed, 7% of Fe and 15% of Cu were lost from the catalyst. Hence, it can be stated that reduction in Fe and Cu could be also a convincing reason for the reduction of catalytic activity of $CuFe_2O_4$.

8. UV-Vis Spectra Changes and Mineralization of SY

Fig. 8(a) shows the temporal evolution of spectral changes during SY degradation by PMS/$CuFe_2O_4$/US. It is simply seen that the diminishment of the absorption bond of SY at 482 nm was because of azo links fragmentation via free radicals. Furthermore, the reduction of the absorbance at 228 and 314 is evaluated as the sign of degrading aromatic fragment in the dye molecule and its intermediates [40]. Indeed, the peaks of 228 nm and 314 nm were mainly caused by naphthalene and benzene rings, respectively. Moreover, a new peak at 246 nm is associated with some intermediates formed during the reaction. These products probably were non-degradable intermediates resulting from the degradation of naphthalene and benzene rings. It was obvious that the naphthalene ring and nitrogen to nitrogen double bond (azo bond) of SY were destructed via free radicals. As the reaction proceeded, the intensities of the visible absorption peaks dramatically declined, and the color was faded with time lapses, indicating that $CuFe_2O_4$ and US had satisfactory catalytic activity for PMS. To verify the performance of PMS/$CuFe_2O_4$/US process, the mineralization of SY using TOC analysis was tested. TOC removals are presented in Fig. 8(b). As shown, with increase of reaction time, TOC removal was enhanced. Compared to decolorization, TOC removal (50%) was approximately a half of it at the same reaction time. These results showed that 50%

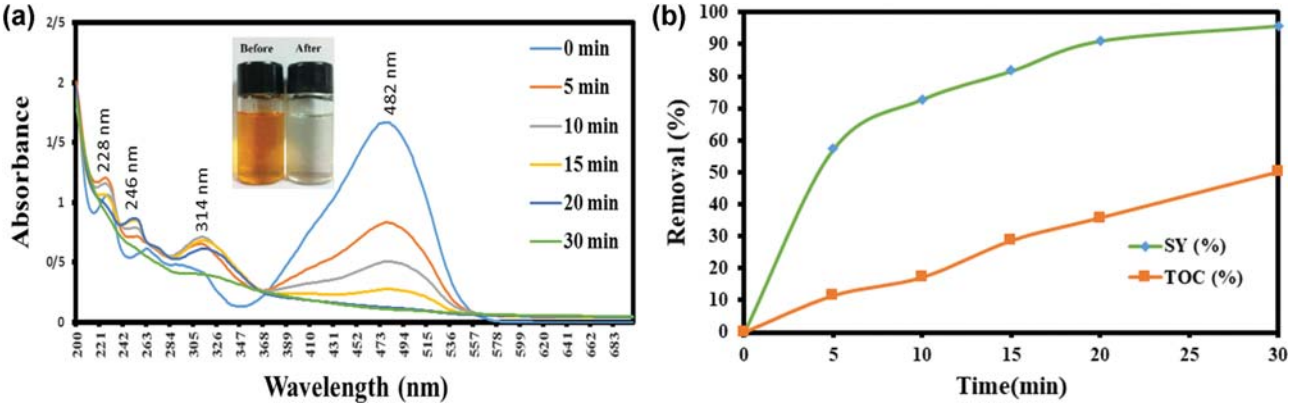

Fig. 8. (a) UV-Vis spectra of SY in the PMS/$CuFe_2O_4$/US process (b) TOC removal of SY in the PMS/$CuFe_2O_4$/US process (SY=50 mg/L, $CuFe_2O_4$=25 mg/L, pH=7, PMS=1.5 mM and US=200 W).

of organic carbon of SY was oxidized to CO_2. According to previous discussions, simultaneous use of US and $CuFe_2O_4$ for PMS activation could effectively degrade SY through synergistic effect (Scheme 1).

CONCLUSIONS

The present study revealed that the combination of US and $CuFe_2O_4$ can effectively activate PMS to generate free radicals for the decolorization of SY. $CuFe_2O_4$ and US demonstrated a considerable activity in PMS decomposition for SY removal in comparison with PS and H_2O_2. The optimal conditions for efficient SY degradation were pH 7.0, PMS 1.5 mM, catalyst loading 25 mg/L, ultrasonic power 200 W and 30 min time. Under the above-mentioned conditions, the decolorization efficiency was 95.8%, while 50% of TOC was removed at the same time. The presence of anions suppressed the performance of US/PMS/$CuFe_2O_4$ especially nitrite ions. Both radical (sulfate and hydroxyl radicals) were equally responsible of dye degradation. Eventually, US/PMS/$CuFe_2O_4$ process might be considered as an efficient and effective process for the destruction of organic dyes in aqueous solution.

ACKNOWLEDGEMENTS

This paper was issued from the thesis of Rouzhan Feizi under grant number ETRC9644. Special thanks to Ahvaz Jundishapur University of Medical Sciences for their financial support.

REFERENCES

1. X. Jin, M.-q. Jiang, X.-q. Shan, Z.-g. Pei and Z. Chen, *J. Colloid Interface Sci.*, **328**, 243 (2008).
2. V. Gupta, *J. Environ. Manage.*, **90**, 2313 (2009).
3. C. D. Raman and S. Kanmani, *J. Environ. Manage.*, **177**, 341 (2016).
4. M. A. Zazouli, F. Ghanbari, M. Yousefi and S. Madihi-Bidgoli, *J. Environ. Chem. Eng.*, **5**, 2459 (2017).
5. D. B. Miklos, C. Remy, M. Jekel, K. G. Linden, J. E. Drewes and U. Hübner, *Water Res.*, **139**, 118 (2018).
6. K.-Y. A. Lin, Z.-Y. Zhang and T. Wi-Afedzi, *J. Water Process Eng.*, **24**, 83 (2018).
7. L. W. Matzek and K. E. Carter, *Chemosphere*, **151**, 178 (2016).
8. B.-T. Zhang, Y. Zhang, Y. Teng and M. Fan, *Crit. Rev. Environ. Sci. Technol.*, **45**, 1756 (2015).
9. D. Zhou, H. Zhang and L. Chen, *J. Chem. Technol. Biotechnol.*, **90**, 775 (2015).
10. M. G. Antoniou, A. A. de la Cruz and D. D. Dionysiou, *Appl. Catal., B*, **96**, 290 (2010).
11. S.-H. Do, J.-H. Jo, Y.-H. Jo, H.-K. Lee and S.-H. Kong, *Chemosphere*, **77**, 1127 (2009).
12. J. A. Khan, X. He, H. M. Khan, N. S. Shah and D. D. Dionysiou, *Chem. Eng. J.*, **218**, 376 (2013).
13. J. Zhang, X. Shao, C. Shi and S. Yang, *Chem. Eng. J.*, **232**, 259 (2013).
14. C. Cai, H. Zhang, X. Zhong and L. Hou, *J. Hazard. Mater.*, **283**, 70 (2015).
15. G. P. Anipsitakis, E. Stathatos and D. D. Dionysiou, *J. Phys. Chem. B*, **109**, 13052 (2005).
16. X. Chen, X. Qiao, D. Wang, J. Lin and J. Chen, *Chemosphere*, **67**, 802 (2007).
17. W.-D. Oh, Z. Dong and T.-T. Lim, *Appl. Catal., B*, **194**, 169 (2016).
18. Y. Ding, L. Zhu, N. Wang and H. Tang, *Appl. Catal., B*, **129**, 153 (2013).
19. W. Tang, Y. Su, Q. Li, S. Gao and J. K. Shang, *Water Res.*, **47**, 3624 (2013).
20. S. Tao, F. Gao, X. Liu and O. T. Sørensen, *Mater. Sci. Eng.: B*, **77**, 172 (2000).
21. X. Zhang, M. Feng, R. Qu, H. Liu, L. Wang and Z. Wang, *Chem. Eng. J.*, **301**, 1 (2016).
22. H. Yang, J. Yan, Z. Lu, X. Cheng and Y. Tang, *J. Alloys Compd.*, **476**, 715 (2009).
23. J. Herney-Ramirez, M. A. Vicente and L. M. Madeira, *Appl. Catal., B*, **98**, 10 (2010).
24. S. R. Pouran, A. A. A. Raman and W. M. A. W. Daud, *J. Clean. Product.*, **64**, 24 (2014).
25. M. Ahmadi and F. Ghanbari, *Environ. Sci. Pollut. Res.*, **25**, 6003 (2018).
26. T. Zhang, H. Zhu and J.-P. Croue, *Environ. Sci. Technol.*, **47**, 2784 (2013).
27. Y.-H. Guan, J. Ma, Y.-M. Ren, Y.-L. Liu, J.-Y. Xiao, L.-q. Lin and C. Zhang, *Water Res.*, **47**, 5431 (2013).
28. K. H. Chan and W. Chu, *Water Res.*, **43**, 2513 (2009).
29. Z. He, L. Lin, S. Song, M. Xia, L. Xu, H. Ying and J. Chen, *Sep. Purif. Technol.*, **62**, 376 (2008).
30. W.-D. Oh, Z. Dong, Z.-T. Hu and T.-T. Lim, *J. Mater. Chem. A*, **3**, 22208 (2015).
31. R. Huang, Z. Fang, X. Yan and W. Cheng, *Chem. Eng. J.*, **197**, 242 (2012).
32. A. Tsitonaki, B. Petri, M. Crimi, H. Mosbæk, R. L. Siegrist and P. L. Bjerg, *Crit. Rev. Environ. Sci. Technol.*, **40**, 55 (2010).
33. X. Feng, G. Mao, F. Bu, X. Cheng, D. Jiang and J. Jiang, *J. Magn. Magn. Mater.*, **343**, 126 (2013).
34. G. P. Anipsitakis and D. D. Dionysiou, *Environ. Sci. Technol.*, **38**, 3705 (2004).
35. Y. Ji, C. Dong, D. Kong and J. Lu, *J. Hazard. Mater.*, **285**, 491 (2015).
36. R. Yuan, S. N. Ramjaun, Z. Wang and J. Liu, *J. Hazard. Mater.*, **196**, 173 (2011).
37. G.-D. Fang, D. D. Dionysiou, Y. Wang, S. R. Al-Abed and D.-M. Zhou, *J. Hazard. Mater.*, **227**, 394 (2012).
38. P. Neta, R. E. Huie and A. B. Ross, *J. Phys. Chem. Ref. Data*, **17**, 1027 (1988).
39. H. Lin, J. Wu and H. Zhang, *Chem. Eng. J.*, **244**, 514 (2014).
40. H. Li, Y. Gong, Q. Huang and H. Zhang, *Ind. Eng. Chem. Res.*, **52**, 15560 (2013).